Numerical study of the magnetized friction force

A. V. Fedotov,[1] D. L. Bruhwiler,[2] A. O. Sidorin,[3] D. T. Abell,[2] I. Ben-Zvi,[1] R. Busby,[2] J. R. Cary,[2,4] and V. N. Litvinenko[1]

[1]*Brookhaven National Laboratory, Upton, New York 11973, USA*
[2]*Tech-X, Boulder, Colorado 80303, USA*
[3]*JINR, Dubna, Russia*
[4]*University of Colorado, Boulder, Colorado 80309, USA*

(Received 14 November 2005; published 7 July 2006)

Fundamental advances in experimental nuclear physics will require ion beams with orders of magnitude luminosity increase and temperature reduction. One of the most promising particle accelerator techniques for achieving these goals is electron cooling, where the ion beam repeatedly transfers thermal energy to a copropagating electron beam. The dynamical friction force on a fully ionized gold ion moving through magnetized and unmagnetized electron distributions has been simulated, using molecular dynamics techniques that resolve close binary collisions. We present a comprehensive examination of theoretical models in use by the electron cooling community. Differences in these models are clarified, enabling the accurate design of future electron cooling systems for relativistic ion accelerators.

DOI: 10.1103/PhysRevSTAB.9.074401 PACS numbers: 29.27.Bd, 41.75.Lx

I. INTRODUCTION

Electron cooling is an extremely useful technique for obtaining high-quality ion beams of high-intensity and low momentum spread [1]. In this method, the phase-space density of an ion beam is increased by means of a dissipative force—the dynamical friction (or velocity drag) on individual ions undergoing Coulomb collisions with a lower temperature electron distribution. We present new computational results, which clarify and resolve large differences between alternate analytical descriptions of the friction force for magnetized electrons.

Cooled ion beams enable experiments under conditions unavailable otherwise, including the generation and storage of rare nuclei and short-lived isotopes, high-precision measurement of lifetimes for radioactive nuclides and of isotope masses, as well as other numerous applications. The profound impact of electron cooling on nuclear, atomic, and molecular physics and future applications of cooled beams has been reviewed [2–4].

A variety of theoretical models for the friction force have been developed [4–10]. However, the available expressions make strong approximations, and the discrepancy between theory and experiments can be large. For existing low-energy coolers, this qualitative description was considered satisfactory.

High-energy electron cooling (i.e. for beams with relativistic parameter $\gamma \gg 1$) can open new possibilities in experimental nuclear physics by producing fundamentally higher-brightness beams in colliders, and is presently considered for the Relativistic Heavy Ion Collider (RHIC) [11] and Facility for Antiproton and Ion Research (FAIR) [12] projects. However, the cooling times at high energy are much longer, making order of magnitude qualitative estimates unacceptable. Quantitative calculation of cooling times requires an accurate description of the cooling force [13].

II. PROBLEMS WITH EXISTING ANALYTICAL MODELS

A theoretical calculation of the energy loss by an ion passing through a cloud of electrons in an external magnetic field has been extensively studied by the plasma community (see, for example, recent Refs. [14,15] and references therein). A treatment is typically done via two complementary approaches: binary-collision model and dielectric linear response treatment.

In the binary-collision model, the energy loss of an ion, due to dynamical friction, is calculated as successive energy transfers due to binary collisions between the ion and electrons. The problem which one encounters in such an approach is a divergent result at large impact parameters, which requires an upper cutoff that is not clearly defined. Also, one cannot account for possible contributions to the friction force from collective plasma oscillations.

In the dielectric linear response approach, an ion is treated as a perturbation to the electron plasma, and energy loss due to friction is caused by the polarization of the surrounding medium. For this approach, the electron plasma is treated as a polarizable fluid, which can be described by the phase-space distribution function of electrons. The evolution of the distribution function is described by the Vlasov-Poisson equation. By solving the linearized Vlasov equation, one can obtain an expression for the induced electric field which is the source of the friction force acting on the ion. This approach also leads to divergent results, but now at small impact parameters, because the linearized theory cannot correctly treat close encounters. However, such a model includes collective phenomena such as plasma oscillations.

In the presence of a finite-strength magnetic field, both treatments have further complications. The binary-collision treatment does not provide a closed form solution anymore, because the relative motion and the center of mass motion are now coupled. Closed form expressions can be obtained only for the limiting case of infinite magnetic field strength. For arbitrary magnetic field strength, numerical simulations are required. In the dielectric treatment, there exists a closed form expression for the friction force, but it requires numerical evaluation of multidimensional integrals with strongly oscillatory integrands [6,10]. A practical expression, in the form of a one-dimensional integral, is possible only in the limit of a very strong magnetic field [5,8].

In recent years, numerical simulations have been used to explore in detail the collisions between ions and magnetized electrons for arbitrary magnetic field strengths [15]. However, to the best of our knowledge, a systematic comparison with the friction force formulas used by the electron cooling community has not been reported. In this paper, we present a systematic comparison between available formulas and simulation results from the VORPAL code [16], which includes a recently implemented algorithm to explicitly resolve close binary collisions [17]. To enable validation of VORPAL results at least for some limiting cases, like the limit of zero and very strong magnetic field, numerical integration over Gaussian electron velocity distributions has been added to the BETACOOL code [18].

III. DESCRIPTION OF THE NUMERICAL APPROACH

When pairwise forces are computed directly for N particles, $O(N^2)$ operations are required for each time step, making this approach prohibitively slow. For typical beam and plasma applications, one would use the electrostatic particle-in-cell approach (PIC) [19,20], where the grid mediates interparticle forces, resulting in O(N) scaling. However, PIC algorithms do not capture the Coulomb collisions that are central to the physics being simulated here.

A specialized 4th-order predictor-corrector algorithm has been developed [21,22] for use with the $O(N^2)$ pairwise field calculations, which tolerates aggressive variation of the time step independently for each particle and, hence, is more efficient than a fixed-time-step tree-based algorithm for $\sim 10^6$ particles or less.

For the simulations presented here, we generalized this predictor-corrector algorithm to accommodate charged particles in a magnetic field [17,23] and implemented it in VORPAL. New positions and velocities for the ith particle are predicted from a Taylor expansion in time, using the following acceleration and its time derivative:

$$\frac{m_i \mathbf{a}_i}{q_i} = \mathbf{v}_i \times \mathbf{B} + \frac{1}{4\pi\epsilon_0} \sum_j \frac{q_j \mathbf{r}_{ij}}{(r_{ij}^2 + r_c^2)^{3/2}} \tag{1}$$

$$\frac{m_i \dot{\mathbf{a}}_i}{q_i} = \mathbf{a}_i \times \mathbf{B} + \sum_j \frac{q_j}{4\pi\epsilon_0} \left[\frac{\mathbf{v}_{ij}}{(r_{ij}^2 + r_c^2)^{3/2}} + \frac{3(\mathbf{v}_{ij} \cdot \mathbf{r}_{ij})\mathbf{r}_{ij}}{(r_{ij}^2 + r_c^2)^{5/2}} \right], \tag{2}$$

where r_{ij} and v_{ij} are the relative positions and velocities of particles i and j, and r_c is the "cloud radius" or "softening parameter," which we typically choose to be zero. The more complicated corrector step follows Ref. [21], except that retaining 4th-order accuracy requires the $\mathbf{v} \times \mathbf{B}$ force to be recalculated with the predicted velocity, and one of the coefficients must be changed for terms that include B.

For high-energy coolers, the interaction between ions and electrons is typically limited by the time of flight through the cooling section. For example, for a cooling section of a length $L = 13$ m and relativistic factor $\gamma = 108$ for the Au^{+79} ions in RHIC [11], such a time of flight in the beam rest frame is $\tau = L/(\beta\gamma c) = 0.4$ ns, which is the value used in simulations presented here. Because this interaction time is less than a plasma period for expected beam frame electron densities, collective electron dynamics play no significant role and one can neglect electron/electron collisions.

In the general case, the subscripts i, j in Eqs. (1) and (2) range over all electrons and ions. To neglect electron/electron and ion/ion interactions, one restricts the subscript i to range only over the ions, while j ranges over the electrons, and then vice versa.

For all VORPAL simulations presented in this paper, the electron/electron interactions are neglected. For simulations of a single ion interacting with a given electron distribution, this effectively reduces the scaling of the run time from $O(N^2)$ to O(N). Because our simulations typically include of order 10^5 electrons, this change in the scaling is essential to make the problem numerically tractable.

An ion moving through an electron distribution experiences a net velocity drag (the dynamical friction) force, due to Coulomb collisions; however, these collisions also lead to small diffusive changes in the ion velocity vector. The velocity change due to friction increases linearly with the interaction time, while the diffusive changes accumulate in a random walk fashion as the square root of the interaction time. For sufficiently short interaction times, the diffusive velocity changes will completely obscure the velocity drag. For sufficiently long interaction times, the velocity drag will dominate and diffusive effects will be a noiselike perturbation. In a high-energy ion ring, the ions will make many millions of passes through the electron cooling section, so that any diffusive dynamics due to the electrons will be suppressed by a factor greater than 1000 with respect to the friction force.

The VORPAL simulations accurately capture both the friction and the diffusive aspects of the ion velocity changes, but the goal is to determine the dynamical friction

force. For the very short interaction times during a single pass through the cooling section (which is simulated here), the rms spread in the small changes of the ion velocity vector due to diffusion is significant and can be larger than the velocity reduction due to friction. This makes it difficult to accurately extract the friction force from simulated ion velocities. Hence, for each VORPAL data point shown in the figures, corresponding to a single initial ion velocity, we have generated 100's of ion trajectories, N_{traj}, and plotted the mean friction force. According to the central limit theorem, the uncertainty in these mean values is roughly ± 1 rms$/\sqrt{N_{\mathrm{traj}}}$, which is what we have used for the error bars.

IV. FRICTION FORCE WITH ZERO MAGNETIC FIELD

With no magnetic field, the friction force on an ion inside a uniform density electron plasma with velocity distribution function $f(v_e)$ is given by [24]

$$\vec{F} = -\frac{4\pi n_e e^4 Z^2 L}{m} \int \frac{\vec{V}_i - \vec{v}_e}{|\vec{V}_i - \vec{v}_e|^3} f(v_e) d^3 v_e, \qquad (3)$$

where Z is the ion charge number, e is the electron charge, n_e is the electron density, m is the electron mass, V_i and v_e are the ion and electron velocity, and L is the Coulomb logarithm $L = \ln(\rho_{\max}/\rho_{\min})$, where $\rho_{\max}$ and $\rho_{\min}$ are the maximum and minimum impact parameters, respectively. In the general case, an anisotropic velocity distribution (typical situation for electron coolers) can be approximated by a Maxwellian distribution with different temperatures for the longitudinal and transverse degrees of freedom. Simple asymptotic expressions for the case when the transverse rms velocity spread of electrons $\Delta_{e,\perp}$ is much larger than the longitudinal one $\Delta_{e,\parallel}$ have been obtained [5]. They agree within a factor of 2 with direct numerical integration of Eq. (3).

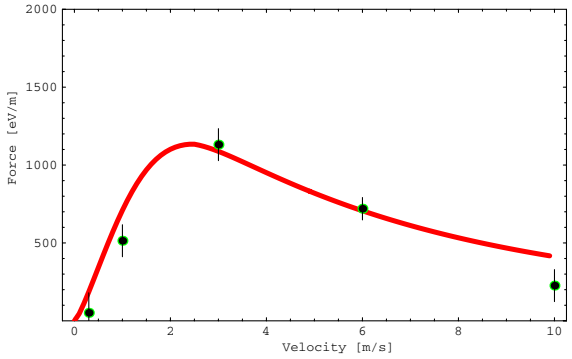

FIG. 1. (Color) Nonmagnetized force (eV/m) vs ion velocity ($\times 10^5$ m/s) for an anisotropic velocity distribution: solid line—Eq. (3) implemented in BETACOOL; points with error bars—simulations using VORPAL.

If an accurate force description is required, and the criterion $\Delta_{e,\perp} \gg \Delta_{e,\parallel}$ is not satisfied, the friction force components can be accurately calculated using numerical evaluation of the integral in Eq. (3). A comparison of VORPAL simulations with the integration of Eq. (3) implemented in BETACOOL (solid line), for the case of an anisotropic Maxwellian distribution of electrons $f(v_e)$ with the rms velocity spreads of $\Delta_{e,\perp} = 4.2 \times 10^5$ and $\Delta_{e,\parallel} = 1.0 \times 10^5$ m/s ($Z = 79$, $n_e = 2 \times 10^{15}$ m^{-3}), is shown in Fig. 1. We find agreement between VORPAL simulations and numerical integration of Eq. (3) to be satisfactory for this and other benchmark tests of zero magnetic field with a typical difference of 10%–20%, depending on the parameters.

V. FRICTION FORCE WITH FINITE MAGNETIC FIELD

The presence of a longitudinal magnetic field changes the collision kinetics, because it limits the transverse motion of electrons. In the limit of a very strong magnetic field, the transverse degree of freedom does not take part in the energy exchange, because all collisions are adiabatically slow relative to the electron Larmor oscillations. In this limit, the friction force is independent of the transverse electron velocities and, hence, is limited only by their longitudinal velocity spread. In typical low-energy electrostatic coolers, the longitudinal electron velocity spread is much smaller than the transverse. The combination of this velocity anisotropy with a moderate longitudinal magnetic field can greatly enhance the longitudinal friction force and provide fast magnetized cooling. In applications to high-energy cooling, this advantage is somewhat reduced, because imperfections in the longitudinal field of a realistic solenoid magnet can lead to a significant increase in the effective velocity spread of electrons. For example, in the magnetized cooling concept for the RHIC-II cooler [25], making the optimistic assumption of longitudinal magnetic field imperfections with an rms distribution of angles at the level of 10^{-5} radians, the effective angular spread of electron trajectories in the beam frame becomes rather large, of order 10^{-3} radians, due to the large relativistic factor $\gamma = 108$.

Expressions for the friction force in the presence of magnetized electrons, based on the dielectic linear response of a plasma, were carried out by Derbenev and Skrinsky [6,7]. The final results of the derivation were also summarized in Refs. [5–8], including the presentation of collision integrals but leaving out specifics of how these integrals were evaluated. As a result, the analysis presented in Ref. [5] is typically referred to as a binary-collision model, even though these integrals were actually evaluated using the dielectric plasma response approach [6,26]. A general treatment based on the dielectric approach was later reported in Refs. [9,10]. Reference [10] also discusses

complications arising in numerical evaluations of the integrals.

In the limiting case of a very strong magnetic field, one can obtain a practical expression, in the form of a one-dimensional integral. Such a result for the magnetized friction force was first obtained by Derbenev and Skrinsky [5,6]:

$$\vec{F} = -\frac{2\pi n_e e^4 Z^2}{m}\frac{\partial}{\partial \vec{V}}\int\left[\frac{V_\perp^2}{U^3}L_M + \frac{2}{U}\right]f(v_e)dv_e, \quad (4)$$

where $\vec{V} = (V_\perp, V_\parallel)$ is the ion velocity, and $U = \sqrt{V_\perp^2 + (V_\parallel - v_e)^2}$ is the relative velocity of the ion and an electron "Larmor circle," with transverse electron velocities assumed to be completely suppressed (i.e. approximation of infinite magnetic field). The actual values of the magnetic field and transverse rms electron velocity spread enter only via the cutoff parameters under the Coulomb logarithm, which is defined as $L_M = \ln(\rho_{\max}/\rho_L)$, where $\rho_L = mc\Delta_{e,\perp}/(eB)$ is the radius of Larmor rotation.

The function in Eq. (4) has asymptotes in the region of small ($V \ll \Delta_{e,\parallel}$) and large ($V \gg \Delta_{e,\parallel}$) ion velocities. For example, for $V \gg \Delta_{e,\parallel}$, the electron distribution can be approximated by the delta function, and integration of Eq. (4) gives [5]

$$F_\parallel = -V_\parallel \frac{2\pi n_e Z^2 e^4}{mV^3}\left[\frac{3V_\perp^2}{V^2}L_M + 2\right], \quad (5)$$

$$F_\perp = -V_\perp \frac{2\pi n_e Z^2 e^4}{mV^3}\left[\frac{V_\perp^2 - 2V_\parallel^2}{V^2}L_M\right], \quad (6)$$

which are the expressions describing adiabatic collisions of the magnetized type. Once again, the expressions in Eqs. (5) and (6) were originally derived based on a perturbative treatment of the collective plasma response. It was later argued by Parkhomchuk [27] that one gets slightly different asymptotic expressions (for $V \gg \Delta_{e,\parallel}$) when using the "binary-collision" approach to evaluate the collision integrals:

$$F_\parallel^{\text{b.c.}} = -V_\parallel \frac{2\pi n_e Z^2 e^4}{mV^3}\left[\frac{2V_\perp^2}{V^2}L_M\right], \quad (7)$$

$$F_\perp^{\text{b.c.}} = -V_\perp \frac{2\pi n_e Z^2 e^4}{mV^3}\left[\frac{V_\perp^2 - V_\parallel^2}{V^2}L_M\right]. \quad (8)$$

In general, one should account for all possible types of collisions such as nonmagnetized (fast), magnetized (adiabatic), and cyclic collisions where the ion can interact several times with the same electron (see, e.g., Ref. [4]). However, in most practical situations for magnetized cooling, any contribution from fast collisions is negligible compared to the adiabatic collisions, since in the fast collisions the relative velocity includes the (much larger) transverse component of the electron velocity. This is true for the parameters of the RHIC cooler discussed in this paper, so we now restrict our attention to the problem of magnetized or "adiabatic" collisions.

Recently, to account for the finite value of the magnetic field, an empirical expression for the magnetized friction force was suggested by Parkhomchuk [28]:

$$\vec{F} = -\vec{V}\frac{4Z^2 e^4 n_e L_p}{m}\frac{1}{(V^2 + \Delta_{e,\text{eff}}^2)^{3/2}}, \quad (9)$$

where $\Delta_{e,\text{eff}}$ is the effective electron velocity spread. The Coulomb logarithm in Eq. (9) is given by

$$L_p = \ln\left(\frac{\rho_{\max} + \rho_{\min} + \rho_L}{\rho_{\min} + \rho_L}\right). \quad (10)$$

Numerical simulations in Ref. [28] showed disagreement with the asymptotic formula of Ref. [5] [i.e. our Eq. (5), with the nonlogarithmic term omitted]. However, the simulations in Ref. [28] assumed perfectly cold electrons, a limit where the friction force actually decreases with increasing magnetic field. The strong disagreement between the cold-electron simulation results in Ref. [28] and the empirical formula being advocated by that work [i.e. our Eq. (9) above] is also confusing.

Furthermore, the possibility of including the nonlogarithmic term in Eq. (5) was not discussed. In fact, the main argument in Ref. [28] against Eq. (5) is that it goes to zero for ion motion along the magnetic field lines (zero transverse ion velocity), which is the case only in the absence of the nonlogarithmic term.

These issues are addressed through VORPAL simulations with both cold and warm electron distributions. We compare our simulation results not just with the asymptotic expressions in Eqs. (5) and (6), but also with the more complete theoretical formula in Eq. (4), from which these asymptotic expressions were obtained. Accurate numerical integration of Eq. (4) has been implemented in the BETACOOL code as well.

VI. FRICTION FORCE SIMULATIONS FOR FINITE MAGNETIC FIELD

A. Longitudinal component of the force

The longitudinal force for the case of zero transverse ion velocity is plotted in Fig. 2. The VORPAL simulations are done for the following parameters: $B = 5$ T, time of interaction in the beam frame $\tau = 0.4$ ns, the rms velocity spreads of the electron beam $\Delta_{e,\perp} = 1.1 \times 10^7$ m/s, $\Delta_{e,\parallel} = 1.0 \times 10^5$ m/s, $Z = 79$, and the density of electrons in the beam frame $n_e = 2 \times 10^{15}$ m^{-3}. It is shown that the friction force expressions, which were constructed based on the asymptotic limits to cover a full range of relative velocities [4] can overestimate force values near the force maximum, which is not surprising since the validity condition for the asymptotic expressions is not satisfied there.

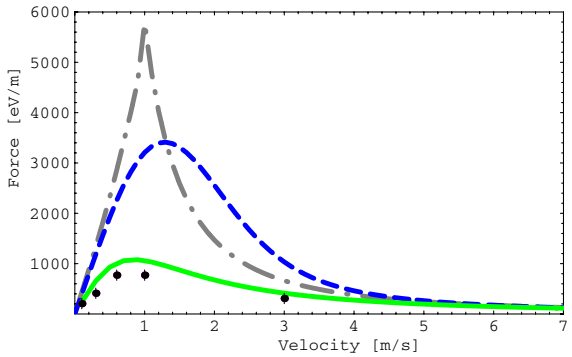

FIG. 2. (Color) Longitudinal component of the force (eV/m) vs ion velocity ($\times 10^5$ m/s). BETACOOL results: solid line (green)—Eq. (9); dot-dashed line (gray)—asymptotics [4]; dashed line (blue)—Eq. (4); VORPAL results: dots with error bars.

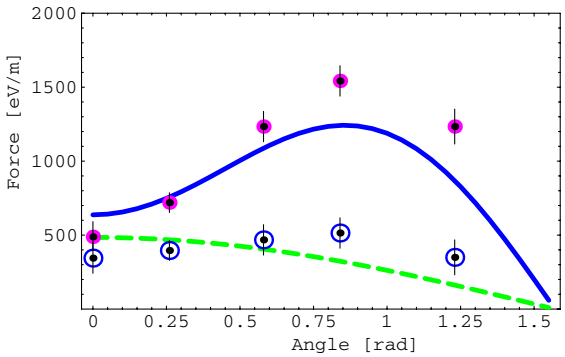

FIG. 3. (Color) Longitudinal component of the force: solid blue line—Eq. (5); dashed green line—Eq. (9); pink dots with error bars—VORPAL results for "cold" electrons; open circles with error bars—VORPAL results for finite-temperature electrons.

The use of Eq. (4) instead of the asymptotic expression helps to avoid an overestimate of the friction force in the vicinity of the longitudinal spread of the electrons. However, the accuracy of the expression in Eq. (4) is itself of a concern since it was obtained with several approximations, including an approximation of a very strong magnetic field. Also, in the limiting case of zero transverse ion velocity (zero angle of the vector of ion velocity with respect to the magnetic field lines), Eq. (4) results in "enhanced" force values compared to VORPAL results or Eq. (9). More details of such a behavior are provided elsewhere [29].

On the other hand, for the same case of zero transverse ion velocity, we find that Eq. (9) is in remarkable agreement with our simulation results. An agreement observed is not unreasonable, because Eq. (9) was obtained through systematic parametric fitting of longitudinal friction force measurements from experiments with ion beams that were already cooled and so had small transverse velocity spread. However, for the design of future high-energy electron coolers, it is extremely important to have an accurate description of the friction force for the initial state of the ion beam, when transverse velocities are still large. Thus, we next consider the longitudinal friction force as a function of the angle between the ion velocity vector and the magnetic field lines.

An important feature of a rigorous description in a strong magnetic field is that, for relative velocities higher than the longitudinal rms electron velocity, the longitudinal and transverse components of the force have very different forms, as can be seen from Eqs. (5)–(8). A dependence on the transverse angle between the ion velocity and the direction of the magnetic field is plotted in Figs. 3 and 4 for the longitudinal component of the friction force and ion velocity $V = 3 \times 10^5$ m/s ($B = 5$ T, $Z = 79$, $n_e = 2 \times 10^{15}$ m^{-3}).

Figure 3 shows (upper curve and points) that the agreement between simulations and Eq. (5) is good if perfectly cold (zero-temperature) electrons are assumed in simulations. However, this "cold-beam" approximation is far from being valid in real situations. Similar dependence of the force on angle was shown by Parkhomchuk using direct numerical computation of the friction force [28]. For finite temperature of the electrons our simulations show even weaker dependence on angle than for the case of the zero-temperature electrons, as shown in Figs. 3 and 4.

Another important property of the magnetized friction force is its dependence on the strength of the magnetic field in the cooling section with the logarithmic increase of the force values with the magnetic field strength being expected. However, numerical simulations reported by Parkhomchuk [28] show a reduction in the friction force as the strength of the magnetic field is increased, which is due to an assumption of zero-temperature electrons. In our simulations with the zero-temperature electrons we confirmed such a dependence on the magnetic field. The reason for such a behavior are the fast collisions which contribution is not suppressed by the electron temperature in this case [29].

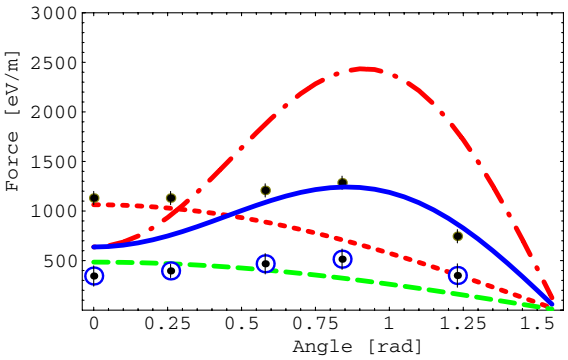

FIG. 4. (Color) Longitudinal component of the force: (1) For $\Delta_{e,\perp} = 4.2 \times 10^5$ m/s: red (dot-dashed) line—Eq. (5); red short-dashed line—Eq. (9); dots with error bars—VORPAL results. (2) For $\Delta_{e,\perp} = 1.1 \times 10^7$ m/s: blue solid line—Eq. (5); green long-dashed line—Eq. (9); open circles with error bars—VORPAL.

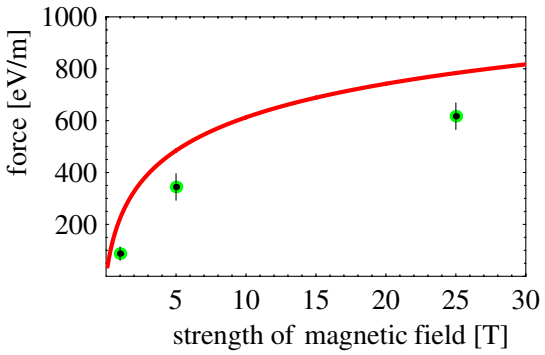

FIG. 5. (Color) Longitudinal friction force (eV/m) for $(V_{\text{ion},\|}, V_{\text{ion},\perp}) = (3 \times 10^5, 0)$ m/s vs magnetic field B (T), for the finite-temperature electron beam with $(\Delta_{e,\|}, \Delta_{e,\perp}) = (1 \times 10^5, 1 \times 10^7)$ m/s. Solid curve—Eq. (9); dots with error bars—VORPAL results.

If the electrons have finite temperature, our simulations show that the friction force increases logarithmically with the magnetic field strength, corresponding to an increased magnetized logarithm, as shown in Fig. 5.

B. Origin of finite longitudinal force at zero transverse angles

Another feature seen in Fig. 3 is the behavior at zero angle (i.e. zero transverse ion velocities), which would lead to zero friction force in the absence of a nonlogarithmic term in Eq. (5). The origin of this constant term in Eq. (5) is due to collective plasma waves [6,7] (see Sec. II for discussion). In a typical low-energy cooler, plasma effects may become important (depending on the parameters) so that inclusion of a term resulting from the collective plasma oscillations is essential. For high-energy coolers, the time of flight of an ion through the cooler in the beam frame becomes extremely short due to the large relativistic factor, so the maximum impact parameter is determined by the finite interaction time rather than dynamic Debye screening.

In our simulations, using parameters of the RHIC cooler, the interaction time in the beam frame is less than one plasma period, which excludes any contribution from plasma waves. Thus the nonlogarithmic term in Eqs. (4) and (5) cannot be justified in our case, so that zero longitudinal friction force at zero transverse angles may be expected for ion velocities much higher than the longitudinal velocity spread of the electrons.

Recently, it was pointed out by Pestrikov [30], that for ion velocities smaller or comparable to the longitudinal velocity spread of the electrons, the integral in Eq. (4) does not go to zero even without the nonlogarithmic term when the transverse velocity of an ion is zero and results in the finite value for the longitudinal component of the force. Such a behavior at zero transverse angle with respect to the magnetic field line is sometimes attributed to the limitation of the approach in which Eq. (4) is derived [29]. For the limiting case of the zero transverse ion velocity, the force value in Eq. (4) without the nonlogarithmic term vanishes completely for the ion velocity equal to $4\Delta_{e,\|}$ or higher.

Simulations with VORPAL show finite friction values at zero angle, even for relatively high ion velocities $V > 4\Delta_{e,\|}$. We attribute these finite force values, in the absence of any collective plasma effects, to incomplete electron-ion collisions, resulting from short interaction times. We also find that this simulated finite longitudinal force scales with the magnetized logarithm, with maximum impact parameter $\rho_{\max}$ determined by the finite interaction time. This is shown in Fig. 4 for $\Delta_{e,\perp} = 4.2 \times 10^5$ m/s ($L_M = 5.6$) and 1.1×10^7 m/s ($L_M = 2.3$). Here, $B = 5$ T, time of interaction in the beam frame is 0.4 ns, $\Delta_{e,\|} = 1.0 \times 10^5$ m/s, $Z = 79$, and the electron density in the beam frame is $n_e = 2 \times 10^{15}$ m^{-3}.

Our conclusion is that the finite friction force, for purely longitudinal ion motion with $V \gg \Delta_{e,\|}$, is due to finite interaction times disrupting the adiabaticity of the magnetized collisions. The nonlogarithmic term in Eq. (4) partially captures this physical effect, although it does not scale correctly with the magnetized logarithm. The parametric model Eq. (9) captures finite values at zero angle quite accurately.

A complete description of the effects of finite interaction times is beyond the scope of this work and will be reported in the near future.

C. Transverse component of the force

For the transverse component of the force, VORPAL simulations show "antifriction" as predicted by the asymptotic formulas in Eqs. (6)–(8). This is shown for the case of an rms electron velocity spread of $\Delta_{e,\perp} = 4.2 \times 10^5$ m/s ($L_M = 5.6$) and 1.1×10^7 m/s ($L_M = 2.3$) in Figs. 6 and 7, respectively. The strength of the antifriction (negative force values on the graphs), as well as the angle value at which the transverse component of the

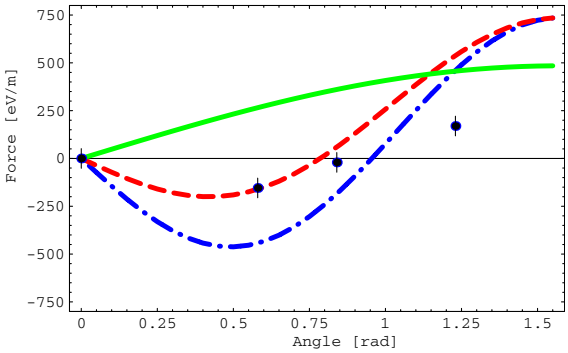

FIG. 6. (Color) Transverse component of the force. Comparison for $\Delta_{e,\perp} = 1.1 \times 10^7$ m/s: blue dot-dashed line—Eq. (6); red dashed line—Eq. (8); green solid line—Eq. (9); dots with error bars—VORPAL results.

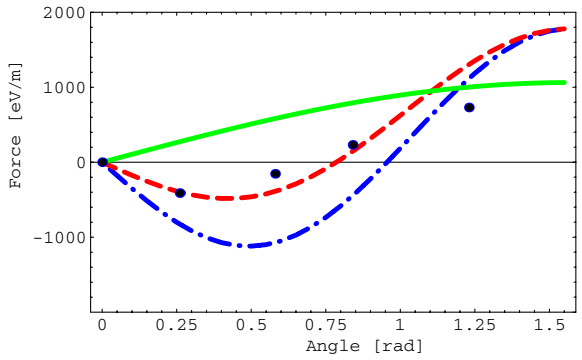

FIG. 7. (Color) Transverse component of the force. Comparison for $\Delta_{e,\perp} = 4.2 \times 10^5$ m/s: blue dot-dashed line—Eq. (6); red dashed line—Eq. (8); green solid line—Eq. (9); dots with error bars—VORPAL results.

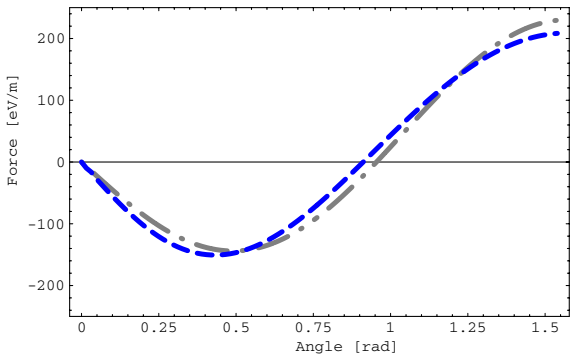

FIG. 9. (Color) Transverse component of the force at ion velocity 6×10^5 m/s ($\Delta_{e,\perp} = 1.1 \times 10^7$ m/s, $\Delta_{e,\parallel} = 1.0 \times 10^5$ m/s, $B = 5$ T): gray dot-dashed line—Eq. (6); blue dashed line—Eq. (4).

friction force changes sign, seems to more closely follow Eq. (8), which was derived using the binary-collision approach [27]. It was argued in Ref. [26] that the difference between the asymptotic expressions in Eqs. (5) and (6), as compared to Eqs. (7) and (8), is caused not by a difference between the dielectric plasma response and binary-collision approaches, but rather by different choices of the cutoff parameters, with the one used in the derivation of Eqs. (7) and (8) judged to be more physical. Equation (9) overestimates transverse friction force at small angles, since it does not show any antifriction.

D. Convergence between asymptotic and numerical results

Note that for our comparison of an angular dependence at $V_{\text{ion}} = 3 \times 10^5$ m/s, with $\Delta_{e,\parallel} = 1 \times 10^5$ m/s, the condition $V_{\text{ion}} \gg \Delta_{e,\parallel}$ is not quite satisfied. The choice $V_{\text{ion}} = 3 \times 10^5$ m/s was made in order to avoid unnecessary problems with numerical accuracy at much larger velocities, for which the friction-induced velocity change becomes extremely small. For example, the force value of 344 eV/m at zero transverse angle in Fig. 3 corresponds to a velocity change of only 0.07 m/s from the initial ion velocity of 3×10^5 m/s in VORPAL simulations. An example of how an asymptotic expression in Eq. (6) and numerical integral in Eq. (4) converge is shown for the ion velocities of 3×10^5 and 6×10^5 (with $\Delta_{e,\parallel} = 1 \times 10^5$ m/s) for the transverse component of the force in Figs. 8 and 9, respectively. For the longitudinal component of the force, one gets similar convergence.

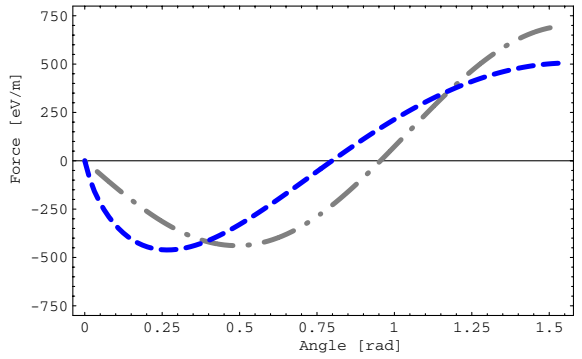

FIG. 8. (Color) Transverse component of the force at ion velocity 3×10^5 m/s ($\Delta_{e,\perp} = 1.1 \times 10^7$ m/s, $\Delta_{e,\parallel} = 1.0 \times 10^5$ m/s, $B = 5$ T): gray dot-dashed line—Eq. (6); blue dashed line—Eq. (4).

VII. DISCUSSIONS

Our computational results show that the asymptotic limits of Eq. (4) given in Eqs. (5)–(8), while useful qualitative guides, are not sufficient for use in electron cooling system design, where an accurate description of the friction force is needed for a large range of relative velocities between the ions and electrons. The use of asymptotic limits to construct a friction force expression to cover a full range of relative velocities [4] leads to an overestimate of the force.

The use of Eq. (4) directly by means of a numerical evaluation of the integral avoids an overestimate of the friction force compared to the asymptotic expressions. However, it requires the use of the nonlogarithmic term (not necessarily justified in some cases) to prevent unphysical behavior at high relative velocities. Also, its functional behavior at zero transverse ion velocity with the enhanced values for the force may be attributed to the limitation of the linearized dielectric approach to treat accurately close collisions.

Equation (9) does not provide a correct description of the magnetized friction force for ion motion at nonzero angles with respect to the magnetic field lines. However, this model overestimates the friction force for some angles, while underestimating it for others. Also, any anisotropy introduced by the magnetic field (ignored by this equation) is very weak for finite-temperature electrons. For a simple estimate of the net cooling power and for finding basic

parameters needed for the cooler, the use of empirical expression in Eq. (9) seems sufficient.

For an accurate description of the friction force in a magnetic field of arbitrary strength, with accuracy better than factor of 2, direct numerical simulations with a code like VORPAL are required.

ACKNOWLEDGMENTS

We thank G. Bell, A. Burov, Ya. Derbenev, P. Messmer, P. Schoessow, P. Stoltz, S. Veitzer, and the Accelerator Physics group of the RHIC Electron Cooling Project for useful discussions. The support of the VORPAL team, and of the Dubna Cooling group with BETACOOL, is greatly appreciated. This work is supported by the U.S. DOE Office of Science, Office of Nuclear Physics under Grants No. DE-FG03-01ER83313, No. DE-FG02-04ER84094, and No. DE-AC02-98CH10886.

[1] G. I. Budker, Atomnaya Energia **22**, 346 (1967).
[2] V. V. Parkhomchuk and A. N. Skrinsky, Rep. Prog. Phys. **54**, 919 (1991).
[3] M. Larsson, Rep. Prog. Phys. **58**, 1267 (1995).
[4] I. N. Meshkov, Nucl. Instrum. Methods Phys. Res., Sect. A **391**, 1 (1997).
[5] Ya. S. Derbenev and A. N. Skrinsky, Part. Accel. **8**, 235 (1978).
[6] Ya. S. Derbenev, Russian Doctorate dissertation, BINP, Novosibirsk, Russia, 1978.
[7] Ya. S. Derbenev and A. N. Skrinsky, Fiz. Plazmy **4**, 492 (1978) [Sov. J. Plasma Phys. **4**, 273 (1978)].
[8] Ya. S. Derbenev and A. N. Skrinsky, *Physics Reviews Vol. 3 (Soviet Scientific Reviews)*, edited by I. M. Khalatnikov (Harwood Academic, New York, 1981), p. 165.
[9] T. Ogino and A. Ruggiero, Part. Accel. **10**, 197 (1980).
[10] A. H. Sorensen and E. Bonderup, Nucl. Instrum. Methods **215**, 27 (1983).
[11] RHIC Electron cooling, http://www.bnl.gov/cad/ecooling
[12] FAIR facility, http://www.gsi.de/GSI-Future/cdr
[13] A. V. Fedotov, I. Ben-Zvi, D. L. Bruhwiler, Yu. Eidelman, V. N. Litvinenko, N. Malitsky, I. N. Meshkov, A. Sidorin, A. Smirnov, and G. Trubnikov, AIP Conf. Proc. **773**, 415 (2005).
[14] O. Boine-Frankenheim and J. D'Avanzo, Phys. Plasmas **3**, 792 (1996), and references therein.
[15] H. B. Nersisyan, G. Zwicknagel, and C. Toepffer, Phys. Rev. E **67**, 026411 (2003), and references therein.
[16] C. Nieter and J. Cary, J. Comput. Phys. **196**, 448 (2004).
[17] D. L. Bruhwiler, R. Busby, A. V. Fedotov, I. Ben-Zvi, J. R. Cary, P. Stoltz, A. Burov, V. N. Litvinenko, P. Messmer, D. Abell, and C. Nieter, AIP Conf. Proc. **773**, 394 (2005).
[18] A. O. Sidorin, I. N. Meshkov, I. A. Seleznev, A. V. Smirnov, E. M. Syresin, and G. V. Trubnikov, Nucl. Instrum. Methods Phys. Res., Sect. A **558**, 325 (2006); http://lepta.jinr.ru.
[19] C. K. Birdsall and A. B. Langdon, *Plasma Physics Via Computer Simulation* (McGraw-Hill, New York, 1985).
[20] P. Messmer and D. L. Bruhwiler, Comput. Phys. Commun. **164**, 118 (2004).
[21] J. Makino and S. J. Aarseth, Publ. Astron. Soc. Jpn. **44**, 141 (1992).
[22] J. Makino, Astrophys. J. **369**, 200 (1991).
[23] R. Busby *et al.*, Bull. Am. Phys. Soc. **48**, 117 (2003).
[24] S. Chandrasekhar, *Principles of Stellar Dynamics* (University of Chicago Press, Chicago, 1942).
[25] V. V. Parkhomchuk and I. Ben-Zvi, BNL Report No. C-AD/AP/47, 2001.
[26] N. S. Dikansky, V. I. Kudelainen, V. A. Lebedev, I. N. Meshkov, V. V. Parkhomchuk, A. A. Sery, A. N. Skrinsky, B. N. Sukhina, BINP Technical Report No. 88-61 (Institute of Nuclear Physics, Novosibirsk, Russia, 1988).
[27] V. V. Parkhomchuk, in *Proceedings of the Workshop on Electron Cooling and Related Applications (ECOOL84, 1984)*, edited by H. Poth, KfK Report No. 3846 (KfK, Karlsruhe, 1985), p. 71.
[28] V. V. Parkhomchuk, Nucl. Instrum. Methods Phys. Res., Sect. A **441**, 9 (2000).
[29] A. V. Fedotov, D. L. Bruhwiler, and A. O. Sidorin, in *Proceedings of the 39th ICFA Advanced Beam Dynamics Workshop HB2006* (KEK, Tsukuba, Japan, 2006).
[30] D. V. Pestrikov, BINP Technical Report No. 2002-57 (Institute of Nuclear Physics, Novosibirsk, Russia, 2002).